

AN ORIGIN OF SUPERSONIC MOTIONS IN INTERSTELLAR CLOUDS

HIROSHI KOYAMA

Astronomical Data Analysis Center,
National Astronomical Observatory, Mitaka, Tokyo 181-8588, Japan;
E-mail address: H.Koyama@nao.ac.jp

AND

SHU-ICHIRO INUTSUKA

Department of Physics, Kyoto University, Kyoto 606-8502, Japan;
E-mail address: inutsuka@tap.scphys.kyoto-u.ac.jp*ApJL in press.*

ABSTRACT

The propagation of a shock wave into an interstellar medium is investigated by two-dimensional numerical hydrodynamic calculation with cooling, heating and thermal conduction. We present results of the high-resolution two-dimensional calculations to follow the fragmentation due to the thermal instability in a shock-compressed layer. We find that geometrically thin cooling layer behind the shock front fragments into small cloudlets. The cloudlets have supersonic velocity dispersion in the warm neutral medium in which the fragments are embedded as cold condensations. The fragments tend to coalesce and become larger clouds.

Subject headings: ISM: clouds — ISM: molecules — ISM: supernova remnants — shock waves — turbulence

1. INTRODUCTION

The interstellar medium (ISM) and cold gas clouds are characterized by a clumpy substructure and a turbulent velocity field (Larson 1981). The maintenance and dissipation processes of the turbulence are supposed to be important in the theory of star formation (McKee 1989, Nakano 1998, Elmegreen 1999). The understanding of the origin of cold clouds and their internal substructure has therefore fundamental importance for a consistent theory of star formation and ISM.

Some of the polarization maps and direct measurements of field strength in some star forming regions suggested the importance of MHD (Alfvén waves) turbulence (Myers & Goodman 1988, Crutcher et al. 1993). Recent simulations of MHD turbulence, however, suggest that it dissipates rapidly (Gammie & Ostriker 1996, Mac Low et al. 1998, Mac Low 1999, Ostriker et al. 1999). Possible sources of energy supply are winds and outflows from young stellar objects (Franco & Cox 1983, McKee 1989). Note however that clumpy structures with supersonic velocity dispersions are also observed even in regions where star formation is inactive. Thus, the origin of clumpy cloud structure remains as an outstanding issue.

We propose that the clumpiness in clouds arises naturally from their formation through thermal instability which acts on timescales that can be much shorter than the duration of the interstellar shocks (e.g., galactic spiral shocks and supernova remnants). The basic properties of the thermal instability are studied in a pioneering paper by Field (1965). Schwarz, McCray, and Stein (1972) studied numerically the growth of condensation in cooling region including the effects of ionization and recombination. Hennebelle & Perault (1999) studied the elementary condensation process in turbulent flow in the restricted conditions of neutral atomic gas in plane-parallel geometry. Burkert & Lin (2000) studied cooling and frag-

mentation of gas using simplified power-law cooling function. Smith (1980) studied collisions between cold atomic clouds, which produce thick layers of shock-heated atomic gas in which thin sheets of cold molecular gas form by the thermal instability. Koyama & Inutsuka (2000, hereafter Paper I) have done one-dimensional hydrodynamic calculations for the propagation of a strong shock wave into warm neutral medium (WNM) and cold neutral medium (CNM) including detailed thermal and chemical processes. They have shown that the post-shock region collapses into a cold layer as a result of the thermal instability. They expect that this layer will break up into very small cloudlets which have different translational velocities.

In this paper, we show that the fragmentation of the shock-compressed layer indeed provides turbulent condensations, by using two-dimensional hydrodynamic calculation with radiative cooling and heating and thermal conduction.

2. NUMERICAL SIMULATIONS

2.1. Numerical Scheme

The hydrodynamics module of our scheme is based on the second-order Godunov method (van Leer 1979). We solve following hydrodynamic equations.

$$\frac{\partial \rho}{\partial t} + \nabla \cdot (\rho \mathbf{v}) = 0, \quad (1)$$

$$\frac{\partial \mathbf{v}}{\partial t} + \mathbf{v} \cdot \nabla \mathbf{v} = -\frac{\nabla P}{\rho}, \quad (2)$$

$$\frac{\partial \rho e}{\partial t} + \nabla \cdot (\rho e \mathbf{v}) + P \nabla \cdot \mathbf{v} = \frac{\rho}{m_{\text{H}}} \Gamma - \left(\frac{\rho}{m_{\text{H}}} \right)^2 \Lambda(T) + \nabla \cdot (K \nabla T), \quad (3)$$

where ρ , P , \mathbf{v} are the density, pressure, and velocity of the gas, the specific internal energy $e = P/(\gamma - 1)\rho$, with $\gamma = 5/3$. m_{H} is the hydrogen mass in gram. Γ

and Λ are heating and cooling rate, respectively. For the coefficient of thermal conductivity we adopt $K = 2.5 \times 10^3 T^{1/2} \text{erg cm}^{-1} \text{K}^{-1} \text{s}^{-1}$ (Parker 1953). Effects of self-gravity and magnetic field are not treated in this paper.

In Paper I, we included the following processes in the hydrodynamic calculations: photoelectric heating from small grains and PAHs, heating and ionization by cosmic rays and X-rays, heating by H_2 formation and destruction, atomic line cooling from hydrogen Ly α , C II, O I, Fe II, and Si II, rovibrational line cooling from H_2 and CO, and atomic and molecular collisions with grains. However the following analytic fitting function adopted here reproduces the features relevant for our purpose:

$$\begin{aligned} \Lambda(T)/\Gamma &= 10^7 \exp(-114800/(T+1000)) \\ &\quad + 14\sqrt{T} \exp(-92/T) \text{cm}^3, \\ \Gamma &= 2 \times 10^{-26} \text{ergs/s}, \end{aligned} \quad (4)$$

where T is in Kelvins.

We use 2048×512 Cartesian grid points covering a 1.44×0.36 pc region so that the spatial resolution is 0.0007 pc = 140 AU.

We have tested the linear growth of the thermal instability (Field 1965). The test is performed with an eigenfunction by using 16 grid points. The numerical results reproduce the linear growth rate with relative errors of 0.05 % when $\delta\rho/\rho < 0.01$

2.2. Initial and Boundary Conditions

To investigate the shock propagation into WNM we consider a plane-parallel shocked layer of gas. We take the y -axis to be perpendicular to the layer. An uniform flow approaches the layer from the upper side with a velocity $V_y = -26$ km/s and density $n = 0.6 \text{cm}^{-3}$ and temperature $T = 6000$ K. We assume that the lower side of the shocked layer is occupied by hot, tenuous gas (density $n = 0.12 \text{cm}^{-3}$) with a high pressure $P/k_B = 4 \times 10^4 \text{Kcm}^{-3}$.

We set up density fluctuations as follows:

$$\frac{\delta\rho(x,y)}{\rho_0} = \frac{A}{k_{\max}} \sum_{i,j=0}^{i_{\max}} (k_i^2 + k_j^2)^{\frac{n}{2}} \sin(xk_i + yk_j + \theta(k_i, k_j)), \quad (6)$$

where $k_i = 2\pi i/L$ is a wave number, θ is a random phase, n is a spectral index, and L is a calculation box size of x -direction. We imposed out-going boundary condition for the y -direction, and periodic boundary condition for the x -direction.

2.3. Results of Thermal Instability and Fragmentation

Figure 1 shows density distribution at $t = 0.337, 1.06$ Myr. We used an initial fluctuation $A = 0.05$, the power index $n = 0$, and $i_{\max} = 16$. Thermally collapsed layer and its fragments are seen in the shock-compressed layers.

Figure 1a shows the beginning of the formation of cold thermally collapsed layer. Density discontinuity at $y \sim 0.46$ pc corresponds to the shock front. Density discontinuity at $y \sim -0.1$ pc is the contact surface between the shock-compressed layer and the hot interior. Behind the shock front, cooling dominates heating and temperature decreases monotonically. The ISM in the range of 300 –

6000 K is thermally unstable. Thus, thermally collapsing layer is subject to thermal instability. The condensations continue to collapse and cool until the radiative cooling balances the radiative heating, in such a way that approximate pressure equilibrium is maintained between condensations and the surrounding gas. Temperature of these clumps finally reaches the value of thermal equilibrium ($T = 20$ K at $n = 2000 \text{cm}^{-3}$). When the cooling balances the heating, the condensation ceases to collapse but the surrounding warm gas continues to cool radiatively and accrete onto the cloud cores.

The cold clumps have considerable translational velocity dispersion. The typical velocity dispersion is about several km/s. The linear analysis predicts that perturbation with sufficiently long wavelength grows exponentially. However, the velocity of the non-linearly developed perturbation has the upper limit that is the sound speed of the warmer medium (≈ 10 km/s), because the driving force of the instability is the pressure of the less dense warmer medium. This non-linearly developed perturbation produces the translational velocities of the cold clumps. These velocity on the order of the sound speed of the WNM is highly supersonic with respect to the sound speed of cold gas. Thus we can understand why the supersonic velocity dispersion of the cold medium is comparable to the sound speed of the WNM.

The cold cloud cools the interface via thermal conduction. The pressure of the warm medium between two cold clumps becomes smaller, which in effect provides an attractive force of two adjacent cold clumps. This attractive force is the driving force of the coalescence of two cold clumps. Thus, cold clumps coalesce into larger clouds.

The sizes of these clumps are a few orders of magnitude smaller than the Jeans length, $\lambda_J = 1.2 \text{pc} \sqrt{(T/20\text{K})(2000 \text{cm}^{-3}/n)}$. Thus, each cloud is gravitationally stable. The shock front itself remains stable at least in 10^6 years in this plane-parallel problem.

For comparison, we changed the initial fluctuations in the range of the amplitude ($A=0.05-0.005$), and the power index ($n=0, \pm 2$), but the resultant velocity dispersion defined by $\int \rho v_{mx}^2 dx dy / \int \rho dx dy$ changed only by 10 %. We also changed the spatial resolution ($512 \times 128, 1024 \times 256$, and 2048×512) but the velocity dispersion changed only by 10 %. Thus, Figure 1 shows a typical result of this problem. From these results we can demonstrate that the role of thermal instability behind the shock front is one of the most important processes in the evolution of interstellar shocked layers.

3. DISCUSSION

3.1. Formation of Molecules

The main coolant in cold dense clouds is supposed to be CO (see, e.g., Neufeld, Lepp, & Melnick 1995; Paper I). H_2 enables the formation of CO and other molecules. The abundance of H_2 in the CNM critically depends on the optical depth and local density. The typical column density of the layer becomes $2 \times 10^{20} \text{cm}^{-2}$. We calculated detailed thermal-chemical equilibrium state in the dense region by adopting the values of density, temperature, and column density from this dynamical simulation. Twenty-five percent of the hydrogen is H_2 and 0.03% of the carbon is CO in thermal and chemical equilibrium.

We simulate the observation of molecular clumps at $t = 1.06$ Myr (Figure 1b) as the Position-Velocity (P-V) diagram of the ^{12}CO $J = 1 - 0$ emission (Figure 2a). We use the usual relationship $T_B = \frac{1}{2}\lambda^2 I/k_B$, with the specific intensity $I = n^2 \Lambda L / (4\pi \Delta v)$, where $n^2 \Lambda$ is the cooling per unit volume, L is the path length, Δv is the Doppler line width. We adopt Δv to be the sound velocity. As shown in Figure 2a, the typical velocity dispersion in the clumps is about a few km/s. The cloud to cloud velocity dispersion is also a few km/s. Figure 2b shows that the P-V diagram of hydrogen nuclei. The velocity dispersion of the diffuse warm medium is about 10 km/s.

3.2. An Origin of “Turbulence” in Interstellar Clouds

Diffuse ISM in the Galaxy is frequently compressed by supernova explosions (McKee & Ostriker 1977). Therefore, the shock propagation into the ISM plays an important role in the evolution of the Galactic ISM. We have studied the shock propagation into WNM by two-dimensional hydrodynamic calculations, and have shown that the thermally collapsed layer breaks up into very small cloudlets. Fragmentation of the thermally collapsing layer is a result of the thermal instability. The thermal instability produces many cloudlets which have different translational velocities. We expect that the Galactic ISM is occupied by these small cloudlets which have supersonic velocity dispersion, because the ISM is frequently compressed by supernova explosions, stellar winds, spiral density waves, cloud-cloud collisions, etc. The H I 21-cm observation maps show the existence of many shell-like or filamentary structures in the Galaxy (Hartmann & Burton 1997). In addition, high resolution observations suggested that the clumpy distribution is ubiquitous in the Galaxy (Heiles 1997). If these structures are really the results of the shock waves, many small molecular cloudlets should be hidden in the shock-compressed layers. These cloudlets should have translational velocities owing to the fragmentation of thermal instability. Observational “turbulence” in the ISM should reflect these motions. Thus, we propose

that an origin of “turbulence” in the ISM is the motion of this small cloudlet complex.

In the radiative shocked layers, the gases lose thermal energy through radiative cooling. Thus, the initial kinetic energy of the pre-shock gas (in the comoving frame of the post-shock gas) converted to the radiation energy, which escapes from the system. If, however, the post-shock gas becomes dynamically unstable by the thermal instability as in this paper, some portion of the thermal energy is transformed into the kinetic energy of the translational motions of the cold cloudlets, which does not easily escape from the system. Therefore we can consider the origin of interstellar turbulence is due to the conversion of the gas energy in supersonic motion. In principle, the kinetic energy of the cloudlets can be lost via coalescence of the cloudlets. The damping rate of the velocity dispersion of the cloudlets will play a key role in the evolution of this system, and hence, should be studied in the subsequent paper.

Expected effects of magnetic field modify the development of the thermal instability described here. The presence of magnetic field can suppress thermal conduction efficiently, allowing the collapse of small scale structure by the thermal instability. The magnetic forces suppress the motion that is perpendicular to the magnetic field lines, and hence suppress the growth of perturbations whose wavevector is perpendicular to the magnetic field lines. However, the magnetic forces do not affect the motion that is parallel to the magnetic field lines, and hence the growth of perturbations whose wavevector is parallel to the magnetic field lines. As a result, the dense sheets or filaments will form and tend to align *perpendicular* to the magnetic field lines. We need three-dimensional calculation to analyze these effects of magnetic fields.

Numerical computations were carried out on VPP300/16R and VPP5000/48 at the Astronomical Data Analysis Center of the National Astronomical Observatory, Japan.

REFERENCES

- Burkert, A., & Lin, D. N. C. 2000, ApJ, 537, 270
 Crutcher, R.M., Troland, T. H., Goodman, A. A., Heiles, C., Kazes, I. & Myers, P. C. 1993, ApJ, 407, 175
 Elmegreen, B. G. 1999, ApJ, 527, 266
 Field, G. B. 1965, ApJ, 142, 531
 Franco, J., & Cox, D. P. 1983, ApJ, 273, 24
 Gammie, C. F. & Ostriker, E. C. 1996, ApJ, 466, 814
 Hartmann, D., & Burton, W. B. 1997, Atlas of Galactic Neutral Hydrogen (Cambridge: Cambridge Univ. Press)
 Heiles, C. 1997, ApJ, 481, 193
 Hennebelle, P. & Perault, M. 1999, A&A, 351, 309
 Koyama, H., & Inutsuka, S. 2000, ApJ, 532, 980 (Paper I)
 Larson, R. B. 1981, MNRAS, 194, 809
 Mac Low, M.-M., Klessen, R. S., Burkert, A., & Smith, M. D. 1998, Phys. Rev. Lett., 80, 2754
 Mac Low, M.-M. 1999, ApJ, 524, 169
 Myers, P. C. & Goodman, A. A. 1988, ApJ, 326, L27
 McKee, C. F. 1989, ApJ, 345, 782
 McKee, C. F. & Ostriker, J. P. 1977, ApJ, 218, 148
 Nakano, T. 1998, ApJ, 494, 587
 Neufeld, D. A., Lepp, S. & Melnick, G. J. 1995, ApJS, 100, 132
 Ostriker, E. C., Gammie, C. F. & Stone, J. M. 1999, ApJ, 513, 259
 Parker, E. N. 1953, ApJ, 117, 431
 Schwarz, J., McCray, R., & Stein, R. 1972, ApJ, 175, 673
 Smith, J. 1980, ApJ, 238, 842

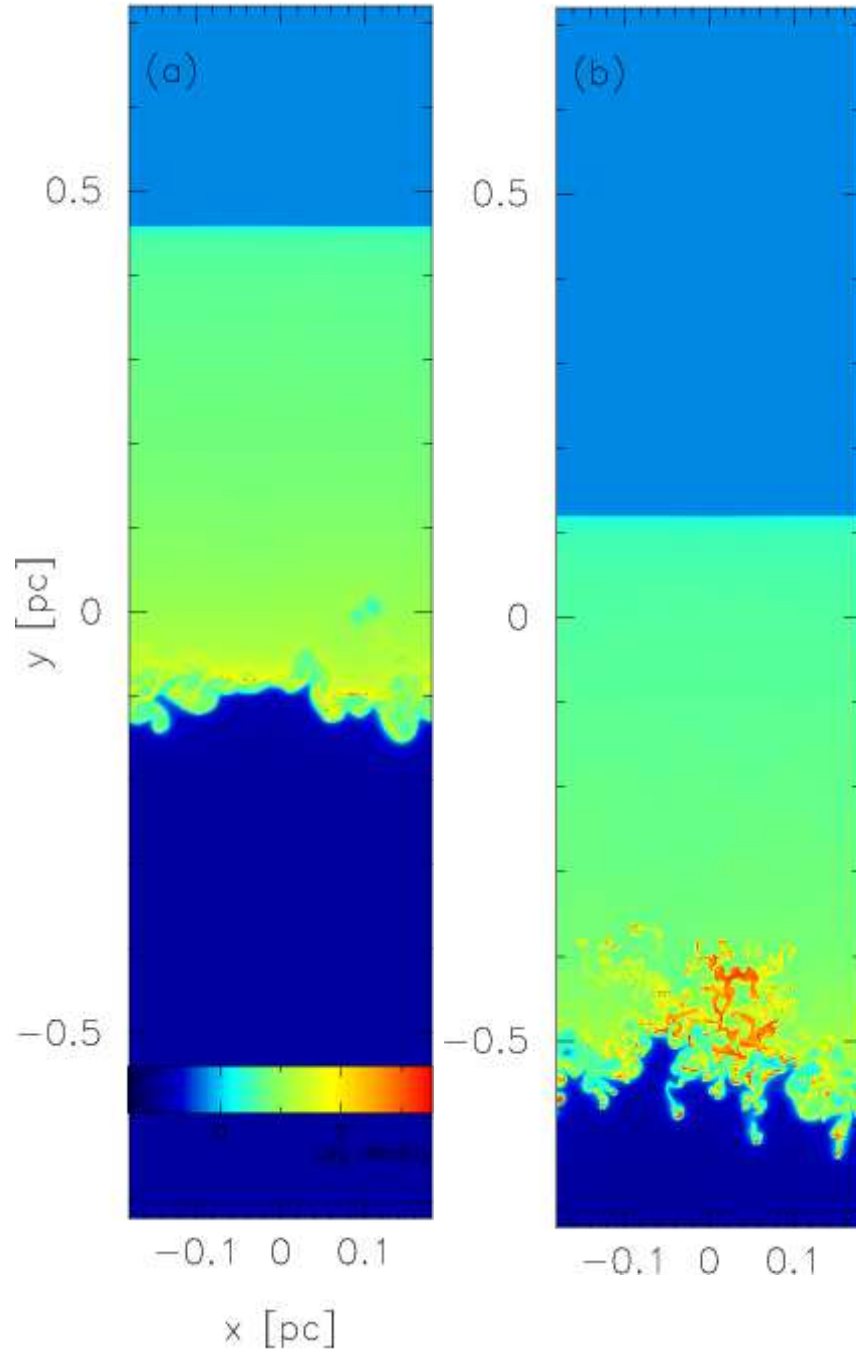


FIG. 1.— Density distribution of the shock-compressed layers. The figures show the snapshot at (a) $t = 0.337$ Myr, (b) $t = 1.06$ Myr, respectively.

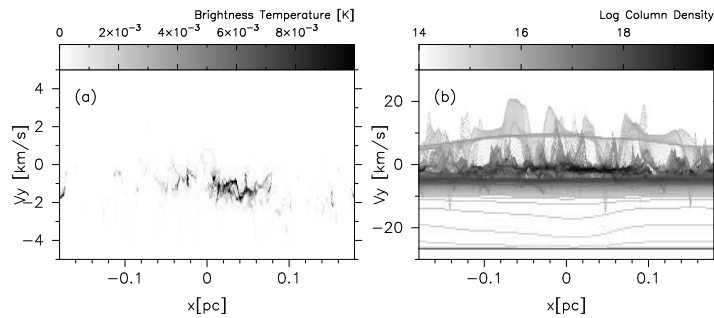


FIG. 2.— The panel a shows the position-velocity (P-V) diagram of the ^{12}CO $J=1-0$ emission obtained from the calculation at $t = 1.06$ Myr (see Figure 1b). We assume 0.03 % of the carbon is CO. The panel b shows the P-V diagram of the hydrogen nuclei.